COMPARATIVE STUDY OF DIFFERENT COILS FOR THE LHC MAIN DIPOLES

S. Russenschuck
CERN, 1211 Geneva 23, Switzerland

Abstract
Two alternative dipole coil cross-section with 6 blocks were found using a new optimization algorithm based on genetic optimization algorithms and the concept of niching. Characteristic of these algorithms is that a number of local optima are found which can then be compared in detail with respect to the objectives such as flexibility, manufacturability and sensitivity to tolerances. The results of this investigations which led to the selection of the v6-1 coil design as the LHC standard coil are presented in this report.

1 Introduction

The superconducting dipoles are characterized by the dominance of the coil geometry for the field distribution. Therefore, the design computations start by optimizing the coil geometry in two and three dimensions, using analytical integration for computing the magnetic field. Contradictory parameters such as maximum dipole field, minimum content of unwanted multipoles and sufficient safety margin for the conductor must be optimized. The keystoning of the conductors and the grading of the current densities between the two layers complicate the task of finding the best solution.

The 5 block dipole coil cross-section which was previously optimized using only deterministic optimization techniques and which is described in the "White Book" [1] project report, has been subject to a number of changes, e.g. change of ground plane insulation, change of insulation thickness (from kapton plus glass epoxy to all kapton) sions, and change of yoke radius i.e. change from separate collars with 180 mm beam separtation distance to racetrack collars with 197 beam separtation. This resulted in the slightly modified version presented in the "Yellow Book"[2]. Since then a change of cable dimensions and a part compensation of the persistent current multipoles resulted in the so-called October 96 version of the "Yellow Book". This design turned out to be too inflexible to accommodate further adjustments if they become necessary at a later stage. In particular a further compensation of the b_3 term (if required) would be difficult due to geometrical constraints, i.e. copper wedges becoming too small at the inner edge. Moreover, the performance of the magnets with the 5 block coil version seems to indicate that the force distribution in the inner block of the inner layer with its 4 turns and an adjacent copper wedge of large dimensions is not very favourable. The search for an alternative was therefore driven by the following objectives:

- Gain more flexibility for further adjustments if they become necessary.
- Aim for symmetric wedges in order to avoid assembly errors and to avoid torque on the wedges due to the electromagnetic forces.
- Increase the quench margin.
- Lower the b_{11} component.
- Find a design with less superconducting material, using genetic optimization algorithms with the concept of niching [3]

Two alternative solutions with 6 blocks were found using a new optimization algorithm based on genetic optimization algorithms and the concept of niching. Characteristic of these algorithms is that **a number** of local optima are found which can then be compared in detail. This is important as not all the objectives e.g. flexibility, manufacturability and sensitivity to tolerances can be considered in the objective function.

2 Electromagnetic properties

Two 6 block coil designs were found to be promising and were studied in detail. They are shown in Fig. 2 and 3 The "October 96" cross-section is shown in Fig. 1. Table 1 gives the cable characteristic data for the inner and outer layer. Table 2 gives the multipole content for the three designs which were studied in detail. **The saturation induced field errors have to be added and the effect of saturation on the load line have to be considered [6].** The persistent currents were calculated by Rob Wolf [7]. The mulitpole content is given in units of 10^{-4} at a radius of 10 mm.

	Outer Layer	Inner Layer
Cable Height (mm) (ins.)	15.4	15.4
Cable inner width (mm) (ins.)	1.6197	1.9728
Cable outer width (mm) (ins.)	1.8604	2.3073
Cable height (mm) (bare)	15.10	15.100
Cable inner width (mm) (bare)	1.362	1.736
Cable outer width (mm) (bare)	1.598	2.064
Radial insulation thickness (mm)	0.150	0.150
Azimuthal insulation thickness (mm)	0.130	0.120
Number of strands	36	28
Diameter of strands (mm)	0.825	1.065
CU/SC Ratio	1.90	1.600
Tref (K)	1.90	1.900
Jc(9.0 T,Tref) (A/mm**2)	1953.0	1433.3
dJc/dB (A/mm**2 T)	550.03	500.34

Table 1: Characteristic data for inner and outer layer cables

The V6-1 design has a B_{ss} which is about 0.1 T higher than in the October 96 version. This is remarkable as it can be achieved with 1 turn less. The explanation is the reduced peak-field to main-field ratio in the inner layer. At the same time the margin in the outer layer blocks is reduced with respect to the October 96 version but still higher than for the inner layer. The b_{11} is considerably reduced. The radial forces on the two inner turns (turn 39 and 40 for the V6-1 version) are reduced. However, the margin in the outer layer is slightly reduced with respect to the Y design. The v6-3 design which uses 3 turns less than the Y solution has an increased margin in the outer layer but the Bss is slightly lower because of limitations in the inner layer.

	V6-3	V6-1	Y
	6 Block (-3 turns)	6 Block (-1 turn)	October 96 (41 turns)
Turns (coil)	38	40	41
Turns inner	16	15	15
Turns outer	22	25	26
% on LL outer	81.05	84.92	82.5
% on LL inner	86.15	85.64	86.5
PF / MF outer	0.83	0.89	0.87
PF / MF inner	1.03	1.03	1.052
I nom (A) (8.36T)	11879.	11532.	11224.
B ss (T)	9.70	9.76	9.65
L (mH/m)	6.64	7.17	7.47
b_3 (pers)	-4.265 / -12.32	-3.817 / -11.03	-4.326 / -12.503
b_5 (pers)	0.193 / 1.611	0.143 / 1.19	0.191 / 1.596
b_7 (pers)	-0.025 / -0.599	-0.0198 / -0.479	-0.034 / -0.819
b_9 (pers)	0.003 / 0.201	0.0033 / 0.229	0.0065 / 0.456
b_{11} (pers)	0.0004 / 0.083	0.0002 / 0.035	0.0007 / 0.147
b_3 (geo)	0.943 / 2.727	1.434 / 4.145	0.107 / 0.309
b_5 (geo)	-0.198 / -1.654	-0.1055 / -0.881	-0.192 / -1.605
b_7 (geo)	0.0122 / 0.249	0.0255 / 0.615	0.0342 / 0.826
b_9 (geo)	-0.0087 / -0.609	0.0014 / 0.101	-0.010 / -0.711
b_{11} (geo)	0.0037 / 0.748	0.0029 / 0.598	0.0088 / 1.774
Pole angle (deg)	70.5	70.99	57.4
Pole size (mm)	7.1	7.43	8.7
Fp (N/m)	16400.	17239.	33877.
Symm wedges	partly	no	no

Table 2: Characteristic data for the three designs. Fp = Electromagnetic force parallel to broad face of cable on first turn in inner layer (ROXIE numbering 40 in V6-1 design). PF/MF = Peak-field (in the coil) to main-field (in the aperture) ratio. The multipole content is given in units of 10^{-4} at a radius of 10 mm and 17 mm.

3 Random multipole errors

The random multipole errors were calculated using 500 identically distributed random errors on the block positioning and inclination angles, and their radial positions, between + and - 0.05 mm. Analysis of the multipole content of these 500 random magnets yields a normal distribution function where the mean value and the standard deviation σ can be calculated.

The mean relative values are not the expected intrinsic values. This is due to the fact that a perturbation of coil block positions resulting in a shift towards the mid-plane gives a higher field error than a move by the same amount away from the mid-plane. As an example for the v6-1 solution, a shift of block no 2 (conductors 10-25) towards the mid-plane by 0.07 mm results in an a2 component of 0.12198 units whereas a shift of 0.07 away from the mid-plane results in an a_2 component of -0.12055 units. Note that the mean b_3 and b_5 in the v6-1 and v6-3 version show the part compensation of the persisten current multipoles and are therefore not zero.

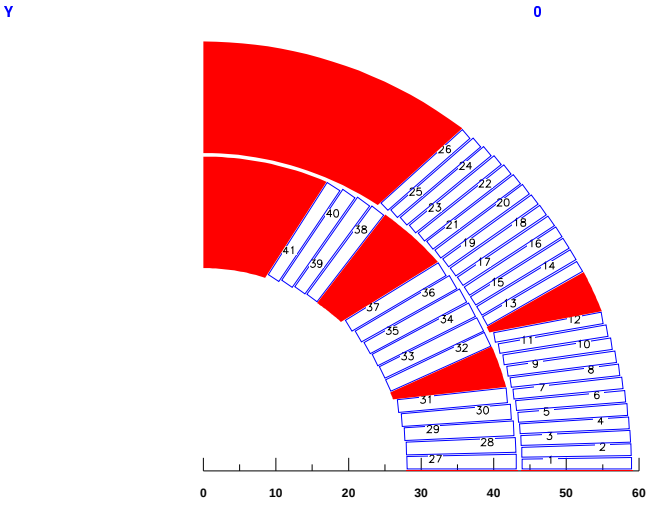

Fig. 1: Coil cross-section for the 5 block (41 turns) modified Yellow-Book design, October 96 solution (Y)

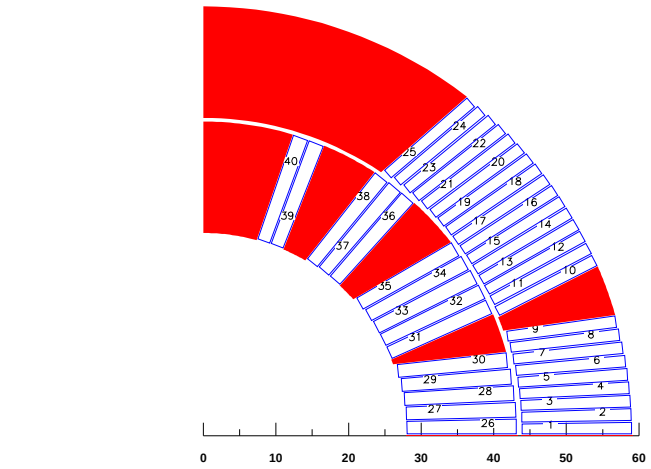

Fig. 2: Coil cross-section for the 6 block (40 turns) design (V6-1). Block numbering as follows: Block 1 = conductors 1-9, Block 2 = conductors 10-25 etc.

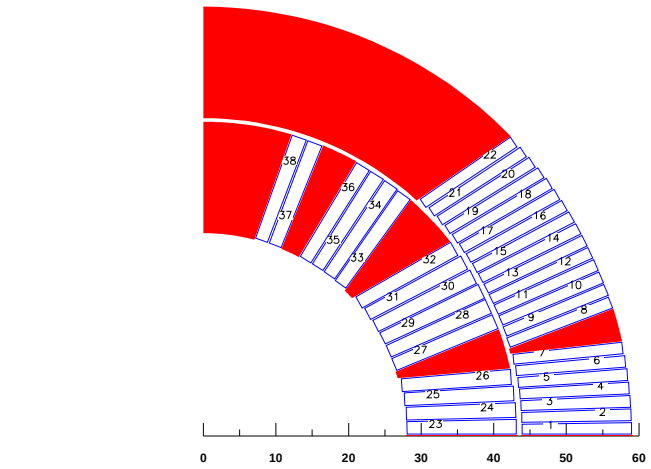

Fig. 3: Coil cross-section for the 6 block (38 turns) design (V6-3)

n	Mean a	Mean b	σ a	σ b
1	-0.00201		1.10912	
2	-0.00257	-0.00678	0.59010	0.57213
3	-0.00998	1.41928	0.24210	0.23534
4	0.00039	-0.00360	0.09055	0.08725
5	-0.00372	-0.10201	0.02939	0.03384
6	-0.00028	0.00017	0.01065	0.01123
7	-0.00014	0.02566	0.00372	0.00388
8	-0.00005	-0.00001	0.00152	0.00103
9	0.00000	0.00140	0.00050	0.00031
10	0.00000	-0.00000	0.00014	0.00014
11	-0.00000	0.00296	0.00004	0.00013

Table 4: Mean values and σ for v6-1 design.
Relative field errors at a radius of 10 mm in units of 10^{-4}.

n	Mean a	Mean b	σ a	σ b
1	0.01514		1.14294	
2	-0.00562	-0.00689	0.63754	0.59091
3	-0.00793	1.49335	0.26552	0.23994
4	0.00179	-0.00357	0.10185	0.09086
5	-0.00367	-0.18082	0.03218	0.03648
6	-0.00027	0.00022	0.01060	0.01262
7	-0.00009	0.01347	0.00360	0.00429
8	-0.00008	-0.00002	0.00154	0.00112
9	0.00000	-0.00174	0.00049	0.00036
10	0.00000	0.00000	0.00014	0.00014
11	-0.00000	0.00290	0.00005	0.00013

Table 5: Mean values and σ for v6-3 design.
Relative field errors at a radius of 10 mm in units of 10^{-4}.

n	Mean a	Mean b	σ a	σ b
1	0.00351		1.81660	
2	0.03028	0.03541	0.74091	0.79640
3	-0.01473	0.05473	0.30395	0.31816
4	-0.00220	0.00247	0.11140	0.11018
5	-0.00130	-0.20189	0.03906	0.04095
6	-0.00013	-0.00026	0.01378	0.01421
7	-0.00030	0.03298	0.00466	0.00510
8	0.00004	0.00003	0.00149	0.00153
9	-0.00002	-0.01030	0.00050	0.00071
10	0.00000	0.00000	0.00015	0.00016
11	0.00000	0.00878	0.00005	0.00039

Table 6: Mean values and σ for the October 96 design. Relative field errors at a radius of 10 mm in units of 10^{-4}.

4 Tuneability

Tables 7 and 8 show the convergence of the optimization algorithm for each design considering the objective

a) to fully compensate all the persistent current effects at injection (b_3 only to 2 units) and

b) no compensation for any effect resulting from persistent currents.

This gives a realistic tuning range to investigate. The objective function F(X) being minimised reads in all cases:

$$F(X) = min((\Delta b_3)^2 + 40(\Delta b_5)^2 + 1000(\Delta b_7)^2 + 9000(\Delta b_9)^2) \quad (1)$$

where $\Delta b_n = b_n - b_n^*$ with b_n the calculated and b_n^* the desired geometrical multipole errors to part compensate the persistent current effects. For the movement of the blocks some limits (constraints) were introduced because of mechanical and geometrical reasons. During the optimization process some of these limits are reached, i.e. the constraints are active. The number of active constraints for a particular design is given in the tables. When the Jacobian matrix is calculated, consisting of the derivatives of the objectives versus the coil positions, the rank of this matrix gives the number of independent base vectors building the design space, i.e. the real number of degrees of freedom to tune the magnet. The rank is calculated with a singular value decomposition of the Jacobian and is given in the table.

	V6-3	V6-1	Y
No. of f. eval.	1501	875	698
F(X)	0.607	0.0557	0.928
b_3* (required)	2.5	2.5	2.5
b_5* (required)	-0.2	-0.15	-0.21
b_7* (required)	0.021	0.022	0.036
b_9* (required)	-0.003	-0.0035	-0.0073
b_3 (achieved)	2.376	2.513	1.85
b_5 (achieved)	-0.241	-0.1602	-0.242
b_7 (achieved)	0.0196	0.026	0.05
b_9 (achieved)	-0.01	-0.003	-0.0129
b_3-b_3*	-0.124	0.0135	-0.65
b_5-b_5*	-0.041	-0.0102	-0.032
b_7-b_7*	-0.0014	0.0040	0.014
b_9-b_9*	-0.0070	0.0005	-0.0056
No. of active constraints	3	3	4
Rank of J	4	3	3

Table 7: Tunability towards a full compensation of the persistent current multipoles at injection

	V6-3	V6-1	Y
Tuning towards	0	0	0
No. of f. eval.	1448	900	628
F(X)	0.331	0.0656	0.398
b_3* (required)	0.	0.	0.
b_5* (required)	0.	0.	0.
b_7* (required)	0.	0.	0.
b_9* (required)	0.	0.	0.
b_3 (achieved)	-0.095	0.0199	-0.102
b_5 (achieved)	-0.033	0.0114	0.016
b_7 (achieved)	-0.0036	0.0044	-0.0011
b_9 (achieved)	-0.005	0.0021	-0.0064
No. of active constraints	4	3	4
Rank of J	4	3	3

Table 8: Tunability towards a zero compensation of the persistent current multipoles at injection

It can be seen that the V6-1 version is tunable in both directions (c.f. the achieved values for F(X)). The Y solution is easier to tune towards 0 compensation than towards full compensation. This is not surprising as originally the 5 block coil design did not feature part compensation of the persistent current effects.

5 Tolerances on cable and insulation size

Taking the tolerances into consideration as given in the technical specifications i.e. +- 0.05 mm for copper wedges, +- 0.006 mm both for the Kapton wrap and the cable size, the multipoles can be calculated for an oversized and undersized coil (worst case). The results for the different designs are given in Table

9. All three designs feature about the same sensitivity, however, v6-1 being slightly less sensitive, especially in the b_5 term.

	V6-3	V6-1	Y
b_3 (coil undersized)	6.40	6.82	5.74
b_3 (coil oversized)	-4.22	-3.74	-5.40
delta b_3	10.62	10.56	11.14
b_5 (coil undersized)	-0.51	-0.356	-0.478
b_5 (coil oversized)	0.029	0.111	0.096
delta b_5	0.539	0.467	0.574
b_7 (coil undersized)	0.039	0.042	0.062
b_7 (coil oversized)	-0.013	0.0052	0.0058
delta b_7	0.052	0.0368	0.0562
b_9 (coil undersized)	-0.0107	-0.0013	-0.015
b_9 (coil oversized)	-0.0045	0.0050	-0.0047
delta b_9	0.0062	0.0063	0.0103

Table 9: Multipole errors for oversized and undersized coils.

6 Mutual inductances

For the calculation of the quench propagation the mutual inductances of the coils are needed, i.e. between upper outer (UO) and upper inner coil (UI) etc. as given in Table 10-12. The self inductances for all 3 designs are given in Table 2. The conclusion from the quench simulation studies is that the 3 designs are very similar from the protection point of view. The maximum layer voltage does not follow the total inductance but mainly the inner layer inductance and the maximum dI/dt, as it is considered that the inner layers stay superconducting (no quench back). From versions v6-1 and v6-3 the preferred one is v6-1 because the outer layer volume is larger. Although the total inductance is higher in the V6-1 version compared to the October 96 version, the maximum temperatures and maximum layer voltages are lower (ref. Minutes of Magnet Bending Working Group no. 8, June 4, 1997, LHC/MMS/DP/4915) [9].

	UO	UI	LI	LO
UO	0.602			
UI	0.221	0.142		
LI	0.140	0.074	0.142	
LO	0.327	0.140	0.221	0.602

Table 10: Mutual inductances for the Y (October 96) design

	UO	UI	LI	LO
UO	0.565			
UI	0.215	0.142		
LI	0.137	0.076	0.142	
LO	0.305	0.137	0.215	0.565

Table 11: Mutual inductances for the V6-1 design

	UO	UI	LI	LO
UO	0.477			
UI	0.204	0.157		
LI	0.133	0.079	0.157	
LO	0.273	0.133	0.204	0.477

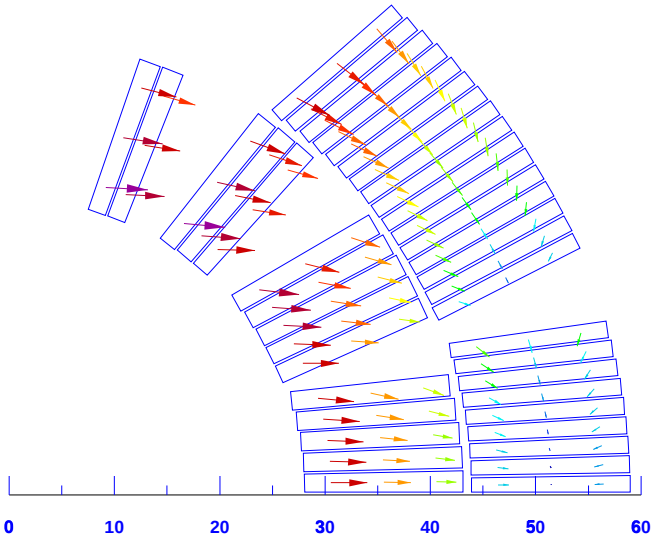

Fig. 4: Force distribution in the v6-1 coil

Table 12: Mutual inductances for the V6-3 design

5

7 EM-Force distribution in the coils

Figures 5-7 show the forces and force distributions for the different magnet design. Fig. 4 gives an impression on the direction of the electromagnetic forces acting on the coil. Fig. 5-7 give the force components per turn for the different coils. The x and y component of the force is displayed together with the component parallel and perpendicular to the broad face of the cable. If the cable is placed in a radial position (inclination angle = positioning angle) these forces correspond to the radial and azimuthal component. The parallel force is defined positive in the outward direction and the perpendicular component positive away from the pole towards the mid-plane of the magnet.

8 Conclusion

The best coil, as far as tunability, margin and sensitivity to tolerances are concerned, is the V6-1 version. The advantages and disadvantages compared to the October 96 version can be summarised as follows:

The advantages are that one turn less results in a more economical design. Further, 0.12 T more central field at quench results in an increased margin to quench due to the reduced peak field to main field ratio in block No. 6. The design also features lower inductance, smaller persistent current effects, smaller $b_1 1$ component, smaller electromagnetic forces parallel to broad sides on first 2 turns, less sensitivity to random errors on wedges and conductor dimensions, better tuneability, and less sensitivity to conductor placement errors on mandrel or collar inner diameter. The 6 block coil also has a more homogeneous force distribution resulting in less shear-stress on the wedge between block 5 and 6 compared to the big wedge between block 4 and 5 in the 5 block coil version.

The disadvantages are that one additional copper wedge in the straight section and one additional end spacer has to be fitted into the coil. The margin to quench of the outer layer is reduced, although

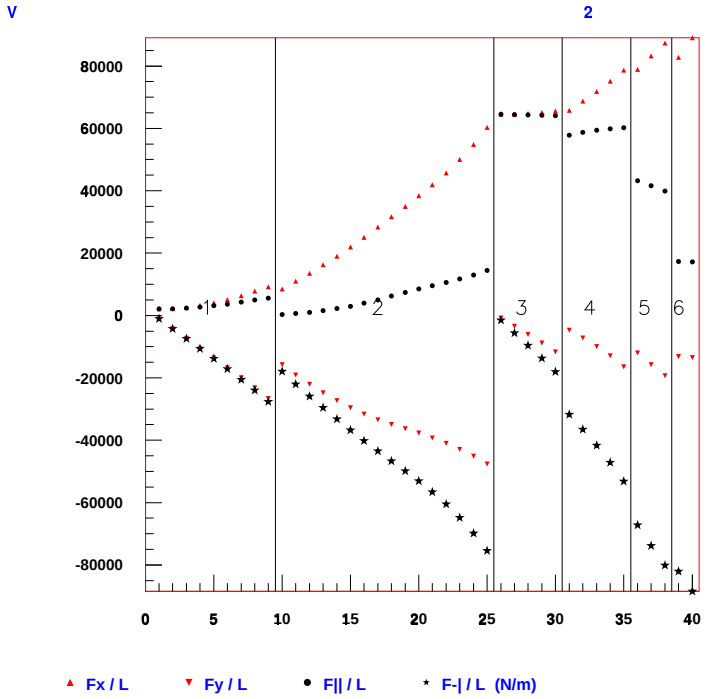

Fig. 5: Forces on each conductor of the V6-1 coil

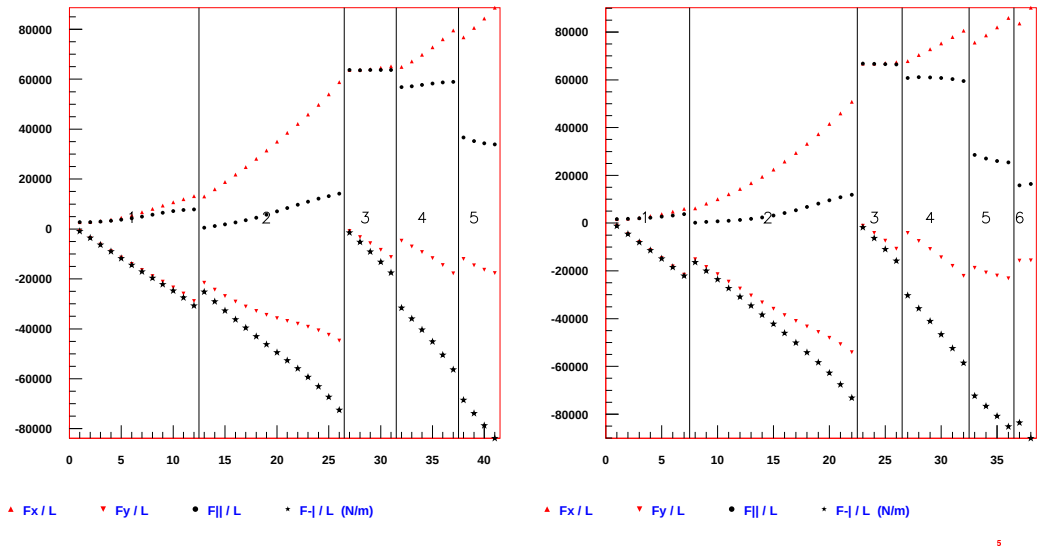

Fig. 6: Forces on each conductor of left: Y coil, right: V6-3 coil

the limiting factor for the short sample current is still the inner layer. The pole angle is smaller in the inner layer of the 6-block version, thus resulting in a smaller bending radius for the inner turn in the end. Winding tests have shown, however, that the cable can be bent around the coil ends in the usual way.

Table 14 gives the position of the coil blocks of the v6-1 coil version. Table 15 gives the geometric multipole content at 17mm in units of 10^{-4} for the coil in a single iron yoke, for the bare coil and for the bare collared coil pair with 194 separtion distance.

Block	No of turns	Radius	pos. angle φ	incl. angle α
1	9	43.900	0.157	0.000
2	16	43.900	21.903	27.000
3	5	28.000	0.246	0.000
4	5	28.000	22.020	24.080
5	3	28.000	47.710	48.000
6	2	28.000	66.710	68.500

Table 14: Position of the coil blocks of the v6-1 coil version.

	Single coil in ctf iron yoke	Bare single coil	2 bare coils in comb. collar
B1	0.0725	0.0598	0.06307
b_2	0.	0.	-89.8151
b_3	4.1454	3.9149	15.5482
b_4	0.	0.	-1.3846
b_5	-0.8813	-1.0384	-0.8337
b_6	0.	0.	-0.0159
b_7	0.6155	0.7456	0.7091
b_8	0.	0.	-0.0001
b_9	0.1010	0.1223	0.1161
b_{10}	0.	0.	0.0000
b_{11}	0.5981	0.7247	0.6876
b_{12}	0.	0.	0.0000
b_{13}	0.0758	0.0918	0.0871

Table 15: Geometric multipole errors at 17 mm in units of 10^{-4} for the coil in a single iron yoke with round collars (coil test facility ctf type, outer yoke radius 98 mm), the bare coil and for the bare collared coil pair (both coils powered) with 194 separtion distance. Current of 100 A.

REFERENCES

[1] CERN, European Organisation for Nuclear Research.: The Large Hadron Collider Accelerator Project, CERN/AC/93-03(LHC).

[2] CERN, European Organisation for Nuclear Research.: The Large Hadron Collider, Conceptual Design, CERN/AC/95-05

[3] Andreev, N.: Internal Note, LHC-MMS 97-02

[4] Ramberger, S., Russenschuck, S.: Genetic algorithms with niching for conceptual design studies, COMPUMAG Rio, 1997

[5] Holland J.H.: Adaption in Natural and Artificial Systems, The MIT Press, Cambridge, 1995

[6] Preis, K., Bardi, I., Biro, O., Magele, C., Renhart, W, Richter, K.R., Vrisk, G.: Numerical analysis of 3d magnetostatic fields, IEEE Transactions on Magnetics, 27, 3798-3803, 1991

[7] Paul, C., Preis, C., Russenschuck, S.: Saturation induced field errors in the LHC main dipoles, LHC-project note 84

[8] Wolf, R.: Private communication

[9] Caspi, S.: Private communication

[10] Rodriguez-Mateos, F.: Private communication